Optimizing Pulse Combustion Parameters in Carbon Anode Baking Furnaces for Aluminum Production

Proceedings of the ASME 2019
International Mechanical Engineering Congress and Exposition
IMECE2019
November 11-14, 2019, Salt Lake City, UT, USA

IMECE2019-10500

OPTIMIZING PULSE COMBUSTION PARAMETERS IN CARBON ANODE BAKING FURNACES FOR ALUMINUM PRODUCTION

Abdul Raouf Tajik[1,2], Tariq Shamim[3,4], Ahmed F. Ghoniem[5], Rashid K. Abu Al-Rub[1,2*]
[1]Mechanical Engineering Department, Khalifa University, P.O. Box 127788, Abu Dhabi, UAE
[2]Aerospace Engineering Department, Khalifa University, P.O. Box 127788, Abu Dhabi, UAE
[3]Mechanical Engineering Department, Northern Illinois University, IL 60115, USA
[4]Mechanical Engineering Program, University of Michigan-Flint, MI 48502, USA
[5]Mechanical Engineering Department, Massachusetts Institute of Technology, Cambridge, MA 02139, USA

ABSTRACT

Pulsating flame jets have been widely used in open-top carbon anode baking furnaces for aluminum electrolysis. Reducing energy consumption and pollutant emissions are still major challenges in baking (heat-treatment) carbon anode blocks. It is also of immense significance to bake all the anodes uniformly irrespective of their position in the furnace. Baking homogeneity can be enhanced noticeably by optimizing anode baking operational, geometrical, and physical parameters. In the present study, CFD simulations are combined with a response surface methodology to investigate and optimize the effects of pulse pressure, pulse frequency, and mainstream inlet oxygen concentration and mainstream inlet temperature. Two-levels half fractional factorial design with a center point is employed. It is perceived that pulse combustion with short pulse time and high momentum results in significant enhancement of the anode baking furnace energy efficiency. The temperature homogeneity is also significantly improved. It is found that the oxygen concentration is statistically the most significant parameter on NOx and soot formations, followed by the fuel flow rate. For NOx formation, air inlet oxygen concentration has a strong interaction with pulse duration. Coupling CFD models with the response surface methodologies demonstrated great potential in multi-objective optimization of the anode baking process with enhanced energy efficiency and baking uniformity.

Keywords: Anode baking furnace; pulse combustion; baking uniformity; oxygen dilution; MILD combustion.

1. INTRODUCTION

Heating by flame jets are widely used in many application, and they are preferred over the induction heating techniques because of their high convective heat transfer, faster heating response time, saving the energy by switching on the burners only when heat is demanded and starting up and cooling down periods are much shorter which also result in energy-saving [1-4]. One of the main challenges in the anode baking process is non-uniform temperature distribution, which results in variability of anodes properties such as electrical resistivity, air, and CO_2 reactivity, thermal shock resistance, and density. This non-homogeneity in the properties of anodes leads to various difficulties in aluminum production, resulting in overconsumption of carbon and energy. Up to a large extent, the baking non-uniformity is due to the non-uniformity in the flue-gas temperature in the flue-wall cavity. In the anode baking process, a specific anode quality has to be achieved while keeping the costs at a minimum. In other words, the fuel consumption and pollutant emissions need to be minimized while simultaneously a particular target gas temperature must be obtained to achieve 100% carbonization of the green anodes. To enhance combustion efficiency and improve carbon anode baking homogeneity [5], a recent development is the use of pulsating flame jets in most of the anode baking furnaces. Several studies are carried out on the application of pulse combustion in several industrial usages [6-7]. It is reported that

* Corresponding author. Tel.: +971-2-810-9162; Fax: +971-2-810-9901
E-mail address: rashid.abualrub@ku.ac.ae, rashedkamel@yahoo.com (R.K. Abu Al-Rub)

pulse combustion leads to heat transfer improvement. In the case of anode baking furnaces, several numerical investigations on anode baking furnace CFD modeling are reported in the literature which due to sizeable computational cost, the pulse combustion is assumed to be continuous [10-15].

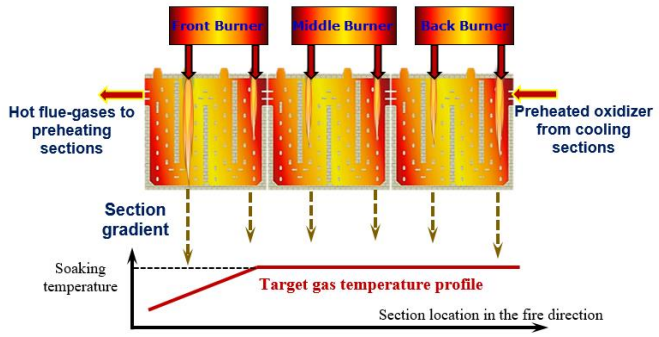

FIGURE 1. BURNER CAPACITY SPLITTING DEPENDING ON THE RAMP LOCATION

Figure 1 shows the location of three burner bridges. The capacity of the burner should be adjusted based on the ramp location by controlling pulse pressure and frequency. Backburners are closer to the cooling sections, and front burners are near the preheating sections. The combustion and emissions characteristics of the pulsating flame jets in the anode baking furnace are relatively less understood. The objective of the present study is to investigate the effect of crucial operational parameters on flow and temperature homogeneity, and energy consumption in the anode baking furnace while employing pulsating flame jets. In specific, the effects of pulse pressure, pulse frequency, air inlet oxygen concentration, and air/fuel ratio are investigated. In the anode baking process optimization, the conventional approaches such as trial and error methods are not cost-effective and fail to provide adequate information on interactions of different input variables. They also fail to provide accurate estimates of the effects and significance level of each factor and to identify clear optimal settings of the factors. In the present study, using a two-level factorial design, the effects of four main furnace operational parameters, namely air inlet temperature, air inlet oxygen concentration, pulse pressure, and pulse duration, are investigated. For full factorial design, sixteen simulations (2^4 = 16) is required. To decrease the required number of simulations from sixteen to eight (2^{4-1} = 8), a half fractional factorial design is considered. Moreover, NOx and soot formations for all eight simulations are estimated.

2. MODEL SPECIFICATIONS

Followings are the main governing equations that are solved to simulate confined turbulent non-premixed combustion in the anode baking furnaces.

2.1. Conservation equations

The equation for conservation of mass, or continuity equation, can be written as follows:

$$\frac{\partial \bar{\rho}}{\partial t} + \nabla.(\bar{\rho}\tilde{\vec{v}}) = 0 \tag{1}$$

Conservation of momentum in an inertial (non-accelerating) reference frame is described by:

$$\frac{\partial\left(\bar{\rho}\tilde{\vec{v}}\right)}{\partial t} + \nabla(\tilde{\vec{v}}.\nabla\tilde{\vec{v}}) = -\nabla p + \nabla.(\bar{\bar{\tau}}) + \bar{\rho}\vec{g} + \vec{F} \tag{2}$$

The stress tensor $\bar{\bar{\tau}}$ is given by:

$$\bar{\bar{\tau}} = \mu\left[\left(\nabla\tilde{\vec{v}} + \nabla\tilde{\vec{v}}^T\right) - \frac{2}{3}\nabla.\tilde{\vec{v}}I\right]$$

2.2. Turbulence modeling

For the conservation equations closure, the Realizable $k-\varepsilon$ model is employed. Followings are the equations for turbulent kinetic energy (k) and its dissipation rate (ε):

$$\frac{\partial\left(\bar{\rho}\tilde{k}\right)}{\partial t} + \bar{\rho}\left(\tilde{\vec{v}}.\nabla\right)\tilde{k} = \nabla.\left[\left(\mu + \frac{\mu_t}{\sigma_k}\right)\nabla\tilde{k}\right] + G_k + G_b - \bar{\rho}\tilde{\varepsilon} - Y_M \tag{3}$$

$$\frac{\partial\left(\bar{\rho}\tilde{\varepsilon}\right)}{\partial t} + \bar{\rho}\left(\tilde{\vec{v}}.\nabla\right)\tilde{\varepsilon} = \nabla.\left[\left(\mu + \frac{\mu_t}{\sigma_\varepsilon}\right)\nabla\tilde{\varepsilon}\right] + \rho C_1 S\tilde{\varepsilon} - \rho C_2\frac{\tilde{\varepsilon}^2}{\tilde{k} + \sqrt{v\tilde{\varepsilon}}} + C_{1\varepsilon}\frac{\tilde{\varepsilon}}{\tilde{k}}C_{3\varepsilon}G_b \tag{4}$$

2.3. Combustion modeling

To estimate the fluctuating characteristics of scalar properties in the turbulent mixing process, the presumed probability density function (PDF) method can be successfully employed. The approach is to assume that the PDF has a certain form in terms of two conserved scalar quantities known as the mixture fraction, f and its variance f', to predict temperature field and species concentrations. A large number of intermediate species and radicals involved in the combustion process can be modeled based on the pre-calculated library as a function of mixture fraction and strain rate.

$$\frac{\partial\left(\bar{\rho}\tilde{f}\right)}{\partial t} + \nabla\cdot\left(\bar{\rho}\tilde{\vec{v}}\tilde{f}\right) = \nabla\cdot\left(\frac{\mu_t}{\sigma_t}\nabla\tilde{f}\right) \tag{5}$$

$$\frac{\partial\left(\bar{\rho}f'^2\right)}{\partial t} + \nabla\cdot\left(\bar{\rho}\tilde{\vec{v}}f'^2\right) = \nabla\cdot\left(\frac{\mu_t}{\sigma_t}\nabla f'^2\right) + C_g\left(\nabla f\right)^2 - C_d\bar{\rho}\frac{\tilde{\varepsilon}}{\tilde{k}}f'^2 \tag{6}$$

2.4. Radiation modeling

In an absorbing, emitting, and scattering medium, the radiative transfer is mathematically described by the radiative transfer equation (RTE) which describes the rate of change of the spectral radiation intensity, I_λ of a radiation beam traveling in the medium at the point r that propagates along a direction, s can be written as:

$$\nabla\cdot\left(I_\lambda\left(\vec{r},\vec{s}\right)\vec{s}\right)=a_\lambda n^2 I_{b\lambda} -\left(a_\lambda+\sigma_s\right)I_\lambda\left(\vec{r},\vec{s}\right)+\frac{\sigma_s}{4\pi}\int_0^{4\pi} I_\lambda(\vec{r},\vec{s}')\phi(\vec{s},\vec{s}')d\Omega' \quad (7)$$

In the present study, the discrete ordinates (DO) radiation model is employed to solve the radiative transfer equation (RTE). The weighted-sum-of-gray-gases model (WSGGM) is employed, which is a reasonable compromise between the oversimplified gray gas model and a complete model which takes into account particular absorption bands.

2.5. NOx modeling

NOx emission consists of mostly nitric oxide (NO), and to a lesser degree of nitrogen dioxide (NO_2) and nitrous oxide (N_2O). NOx is a precursor for photochemical smog, contributes to acid rain, and causes ozone depletion. Mass transport equation is solved for the NO species, considering convection, diffusion, production, and consumption of NO and related species. For thermal and prompt NOx mechanisms, only the NO species transport equation is needed:

$$\frac{\partial\left(\bar{\rho}\tilde{Y}_{NO}\right)}{\partial t}+\nabla\cdot\left(\bar{\rho}\tilde{\vec{v}}\tilde{Y}_{NO}\right)=\nabla\cdot\left(\bar{\rho}D\nabla\tilde{Y}_{NO}\right)+S_{NO} \quad (8)$$

$$\frac{\partial\left(\bar{\rho}\tilde{Y}_{HCN}\right)}{\partial t}+\nabla\cdot\left(\bar{\rho}\tilde{\vec{v}}\tilde{Y}_{HCN}\right)=\nabla\cdot\left(\bar{\rho}D\nabla\tilde{Y}_{HCN}\right)+S_{HCN} \quad (9)$$

$$\frac{\partial\left(\bar{\rho}\tilde{Y}_{NH_3}\right)}{\partial t}+\nabla\cdot\left(\bar{\rho}\tilde{\vec{v}}\tilde{Y}_{NH_3}\right)=\nabla\cdot\left(\bar{\rho}D\nabla\tilde{Y}_{NH_3}\right)+S_{NH_3} \quad (10)$$

Where Y_{NO} is the mass fraction of NO in the gas phase, and D is the effective diffusion coefficient. The source term S_{NO} is to be determined from extended Zeldovich NOx mechanisms.

2.6. Soot modeling

The formation of soot is one of the most complex problems in combustion science, still by far not well understood. However, intense experimental and theoretical research within the last two decades has improved the fundamental understanding and led to a detailed picture of the soot formation process. Soot is commonly believed to be formed by coagulation of polycyclic aromatic hydrocarbon (PAH) species. In the present research, the Brookes and Moss soot prediction model is employed, which is based on two transport equations; one for the radical nuclei concentration and the other for the soot mass fraction. Followings are the governing transport equations:

$$\frac{\partial\left(\bar{\rho}\tilde{Y}_{soot}\right)}{\partial t}+\nabla\cdot\left(\bar{\rho}\tilde{\vec{v}}\tilde{Y}_{soot}\right)=\nabla\cdot\left(\frac{\mu_t}{\sigma_{soot}}\nabla\tilde{Y}_{soot}\right)+\frac{dM}{dt} \quad (11)$$

$$\frac{\partial\left(\bar{\rho}\tilde{b}^*_{nuc}\right)}{\partial t}+\nabla\cdot\left(\bar{\rho}\tilde{\vec{v}}\tilde{b}^*_{nuc}\right)=\nabla\cdot\left(\frac{\mu_t}{\sigma_{nuc}}\nabla\tilde{b}^*_{nuc}\right)+\frac{1}{N_{norm}}\frac{dN}{dt} \quad (12)$$

For pulse combustion, the square wave is used for burners inlet. The square wave is a particular case of a pulse wave which allows arbitrary duration at minimum and maximum. The ratio of the high period to the total period of a pulse wave is called the duty cycle. A true square wave has a 50% duty cycle (equal high and low periods). Note that, for symmetry, the starting time (t = 0) in this expansion is halfway through the first pulse. In the present study, to simulate the on-off operation of the burners, a sinusoidal inlet fuel velocity is considered. Its most basic form as a function of time (t) is:

$$m_{fuel}(t)=A\sin\left(2\pi ft+\varphi\right)=A\sin\left(\omega t+\varphi\right) \quad (13)$$

Where A is the amplitude, f is the ordinary frequency, the number of oscillations (cycles) that occur each second of time, $\omega = 2\pi f$, the angular frequency, the rate of change of the function argument in units of radians per second, φ is the phase, specifies (in radians) wherein its cycle the oscillation is at $t = 0$. It is apparent that there are two parameters that affect fuel consumption, namely the amplitude and the frequency.

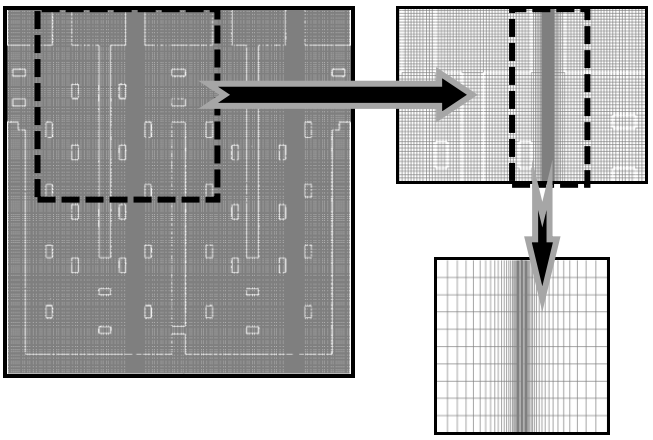

FIGURE 2. COMPUTATIONAL DOMAIN WITH MINIMUM ORTHOGONAL QUALITY = 1.0 AND MAXIMUM ORTHO SKEW = 0

Figure 2 depicts the computational grid. In a view to developing a structured tetrahedral grid, the computational domain is subdivided into hundreds of smaller rectangular elements. The area near the flame is refined to capture the chemical reactions more accurately. A biased factor is considered to avoid a sudden increase in the aspect ratio of the girds. The minimum orthogonal quality is one (orthogonal quality ranges from 0 to 1, where values close to 0 correspond to low quality). The maximum ortho skew quality is zero (ortho skew ranges from 0 to 1, where values close to 1 correspond to low quality). To solve the governing equations, the transient numerical simulations are performed using CFD software (FLUENT 19.2), which is based on finite volume discretization. A comprehensive study is carried to study the sensitivity of the results to different combustion, radiation, and turbulence models. The transient formulation is done based on Second-Order Fully Implicit method. The Second-Order Upwind Scheme is adopted for the spatial discretization. The Semi-Implicit Method for Pressure-Linked Equations (SIMPLE) algorithm is adopted for pressure interpolation and coupling of pressure and velocity. Velocity inlet boundary condition is selected for both fuel and oxidizer streams and pressure outlet for the flow outlet. The spatial and temporal grids independence tests (GIT) are performed. The difference in area-weighted average gas temperature and average species concentrations, after increasing the cell size from 65,000 to 250,000 is found to be less than 1%. The time step size is reduced from 100s to 1s, and the difference is noticed to be less than 0.5%. To ensure a complete convergence, the simulations are initialized with a small time step (0.0001s) and afterward, the time step increased gradually. The optimal time-step size is found to be 0.001s. The residual for all the equations are set to 10^{-6} as the absolute criteria for convergence. The maximum number of iteration for each time step is set to 60 iterations, ensuring a complete convergence for each time step. For the spatial discretization, the First-Order Upwind Scheme is initially adopted and then switched the Second-Order Upwind Scheme.

3. RESULTS AND DISCUSSIONS

The validation of the CFD model is presented in our previous study [14]. In pulse combustion of anode baking furnace, air inlet temperature, inlet oxygen concentration, fuel flow rate, and pulse duration are identified as the key operational parameters to be investigated. In a typical factorial design, the coded values of "+1", "0" and "-1" correspond to the lower, middle and higher levels are considered. For four factors, two-level full factorial design, a total of 17 CFD simulations are required, of which 16 are corner simulations, and one is a center point, to test the quadratic effect. The experiments are costly and challenging. Similarly, CFD simulations of pulse combustion are computationally expensive. Hence, half fractional factorial design can be considered as an alternative, 2^{k-p}. Table 1 provides the coded and un-coded values of the four factors. For instance, the higher value for air inlet oxygen concentration is considered as 23%, and the lower value is chosen as 15%. As shown in Figure 3, the responses are divided into four categories namely (1) temperature values, (2) standard deviation values, (3) uniformity index values, and (4) species concentration values.

TABLE 1. CODED AND UN-CODED VALUES OF THE FOUR FACTORS FOR HALF FRACTIONAL FACTORIAL DESIGN

Run	Coded values for the four factors				Un-coded values for the four factors			
	$Y_{O_2-inlet}$	T_{inlet}	$\dot{m}_f$	t	$Y_{O_2-inlet}$	T_{inlet}	$\dot{m}_f$	t
	(.)	(.)	(.)	(.)	(%)	(°C)	(g/s)	(s)
1	-1	-1	-1	-1	15	1150	2	0.5
2	1	-1	-1	1	23.3	1150	2	1
3	-1	1	-1	1	15	1300	2	1
4	1	1	-1	-1	23.3	1300	2	0.5
5	-1	-1	1	1	15	1150	4	1
6	1	-1	1	-1	23.3	1150	4	0.5
7	-1	1	1	-1	15	1300	4	0.5
8	1	1	1	1	23.3	1300	4	1
9	0	0	0	0	19.15	1225	3	0.75

The aim of optimization of the anode baking process is to meet a target gas temperature, to minimize the standard deviation, to maximize the uniformity index, to minimize fuel consumption, and to minimize pollutant emissions.

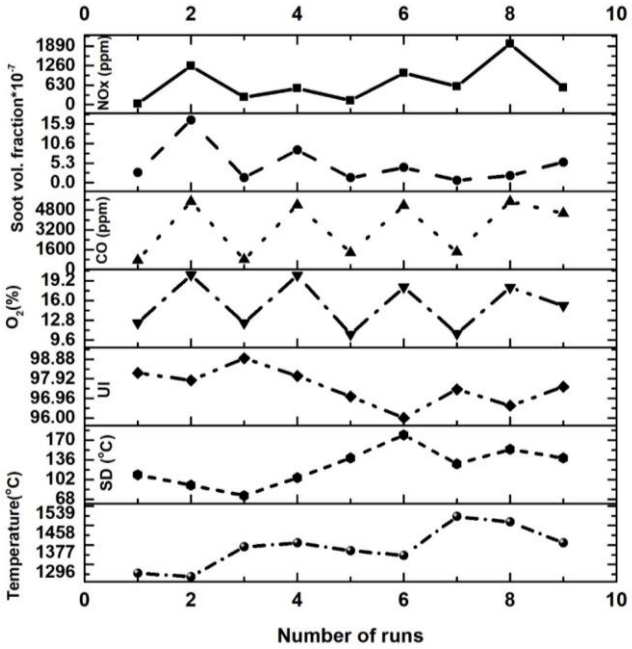

FIGURE 3. RESPONSE VALUES VERSUS RUN NUMBER (SEE TABLE 1)

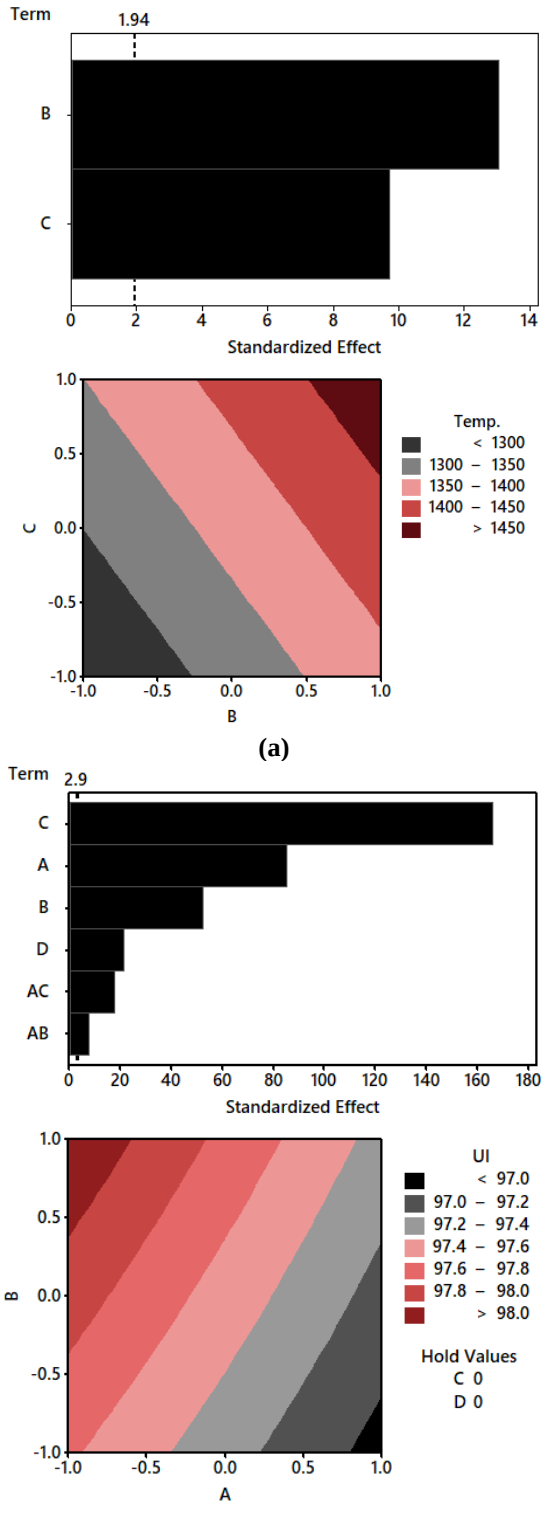

FIGURE 4. SIGNIFICANT MAIN EFFECTS AND THEIR INTERACTIONS FOR A) AVERAGE GAS TEMPERATURE B) GAS TEMPERATURE UNIFORMITY INDEX.

Figure **4** depicts the Pareto charts and contour plots of the standardized effects on average gas temperature and its uniformity index. The backward elimination method is used to retain the significant factors. This method starts with all possible terms in the model and removes the least significant term for each step. The convergence is completed when all variables in the model have p-values that are less than or equal to the specified Alpha to remove the value. The Alpha (α) is considered to be 0.05 corresponds to 95% CI. It can be observed for gas temperature as a response; the air inlet temperature is the most significant factor while the fuel flow rate is the most significant factor for the gas uniformity index as a response.

It can be observed that at lower values of oxygen concentration, the flow uniformity improves. Figure **5** depicts the Pareto charts and contour plots of the standardized effects on soot volume fraction. *A* and *C* are the significant main effects and *AC* is the significant two-way interaction. The interaction effect is evident from the response surface plot.

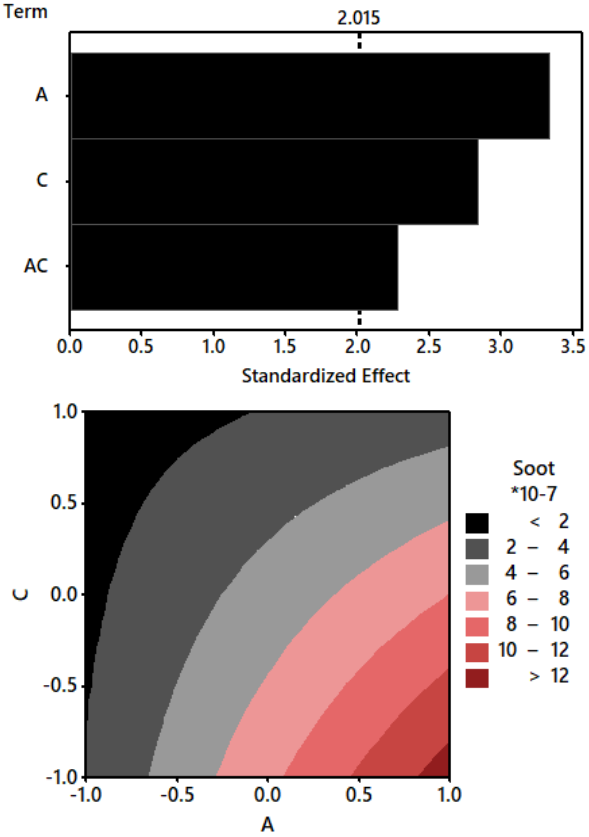

FIGURE 5. SIGNIFICANT MAIN EFFECTS AND THEIR INTERACTIONS FOR SOOT FORMATION.

Figure 6 shows a Pareto chart for NOx concentration showing the significant main effects and two-way interactions. It can be seen that the inlet oxygen concentration is the most significant factor followed by its interaction with factor *D*, which means *AD* is the significant two-way interaction. It can be

remarked from the factorial plot in Figure 6 that by an increase in oxygen concentration, the value of pulse duration dictates the NOx concentration. Fixing the oxygen concentration value at "+1", for the lower pulse duration, the NOx concentration is almost 500 ppm while for the higher pulse duration NOx concentration reaches up to 1500 ppm. Factors C and D have the same level of significance. Thus, it can be perceived that the statistical significance of operational parameters varies drastically for different outputs (response), which should be considered for different optimization scenarios.

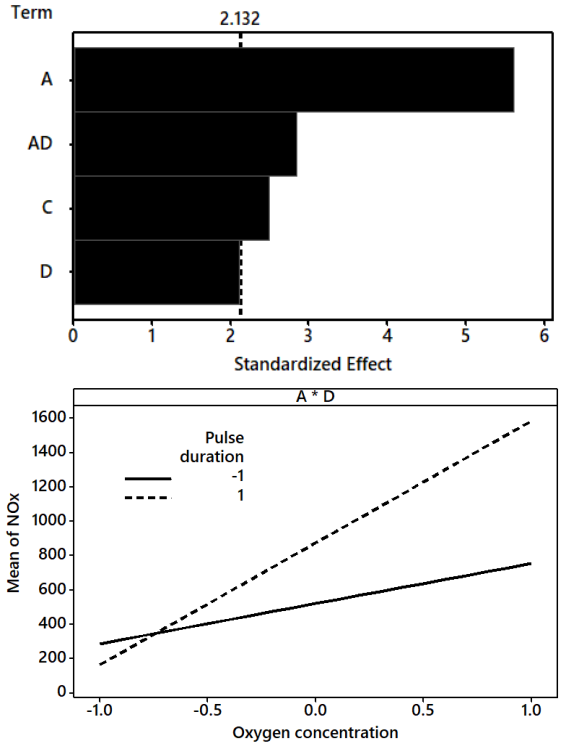

FIGURE 6. SIGNIFICANT MAIN EFFECTS AND THEIR INTERACTIONS FOR NOX FORMATION.

4. CONCLUSIONS

Pulse combustion modeling of an open-top anode baking furnace is performed using RANS formulation equipped with the presumed probability function (PDF) method, the Realizable $k-\varepsilon$ turbulence combustion framework. In the present study, CFD simulations are combined with a response surface methodology to investigate and optimize the effects of pulse pressure, pulse frequency, and mainstream inlet oxygen concentration and mainstream inlet temperature. Two-levels half fractional factorial design with a center point is employed. It is perceived that pulse combustion with short pulse time and high momentum results in significant enhancement of the anode baking furnace energy efficiency. The temperature homogeneity is also significantly improved. It is found that the oxygen concentration is statistically the most significant parameter on NOx and soot formations, followed by the fuel flow rate. For NOx formation, air inlet oxygen concentration has a strong interaction with pulse duration. Coupling CFD models with the response surface methodologies demonstrated great potential in multi-objective optimization of the anode baking process with enhanced energy efficiency and baking uniformity.

ACKNOWLEDGMENTS

The authors acknowledge the financial support provided by the Emirates Global Aluminum (EGA) in UAE under the direction of Dr. Mohamed O. Mahmoud. Also, the authors acknowledge the support and help of the carbon anode team at EGA.

REFERENCES

[1] Hindasageri V, Kuntikana P, Tajik AR, Vedula RP, Prabhu SV. Axis switching in impinging premixed methane-air flame jets. Applied Thermal Engineering. 2016; 107:144-53.

[2] Tajik AR, Kuntikana P, Prabhu SV, Hindasageri V. Effect of the preheated mixture on heat transfer characteristics of impinging methane-air premixed flame jet. International Journal of Heat and Mass Transfer. 2015; 86:550-62.

[3] Kadam AR, Tajik AR, Hindasageri V. Heat transfer distribution of impinging flame and air jets–a comparative study. Applied Thermal Engineering. 2016; 92:42-9.

[4] Tajik AR, Hindasageri V. A numerical investigation on heat transfer and emissions characteristics of impinging radial jet reattachment combustion (RJRC) flame. Applied Thermal Engineering. 2015; 89:534-44.

[5] Meng X, de Jong W, Kudra T. A state-of-the-art review of pulse combustion: Principles, modeling, applications, and R&D issues. Renewable and Sustainable Energy Reviews. 2016; 55:73-114.

[6] Zhonghua W, Mujumdar AS. Pulse combustion characteristics of various gaseous fuels. Energy & Fuels. 2008;22(2):915-24.

[7] Putnam A, Belles F, Kentfield J. Pulse combustion. Progress in energy and combustion science. 1986;12(1):43-79.

[8] Zaidani M, Tajik AR, Qureshi ZA, Shamim T, Abu Al-Rub RK. Investigating the Flue-wall Deformation Effects on Performance Characteristics of an Open-Top Aluminum Anode Baking Furnace. Applied Energy. 2018 Dec 1; 231:1033-1049.

[9] Tajik AR, Shamim T, Ghoniem AF, Abu Al-Rub RK. Multi-objective Optimization of Aluminum Anode Baking Process Employing a Response Surface Methodology. Energy Procedia. 2019 March 15; 158: 5541-5550.

[10] Zaidani M, Abu Al-Rub RK, Tajik AR, Shamim T. Computational Modeling of the Effect of Flue-Wall Deformation on the Carbon Anode Quality for Aluminum Production. In. Proceedings of the ASME's Heat Transfer Summer Conference, Paper No. HT2017-5063, pp. V001T02A010; 11 pages, 2017.

[11] Tajik AR, Shamim T, Zaidani M, Al-Rub RK. The Effects of Flue-Wall Design Modifications on Combustion and Flow Characteristics of an Aluminum Anode Baking Furnace-CFD Modeling. Applied Energy. 2018 Nov 15; 230:207-219.
[12] Tajik AR, Shamim T, Al-Rub RK, Zaidani M. Two-Dimensional CFD Simulations of a Flue-wall in the Anode Baking Furnace for Aluminum Production. Energy Procedia. 2017 May 31; 105:5134-9.
[13] Tajik AR, Al-Rub RK, Zaidani M, Shamim T. Numerical Investigation of Turbulent Diffusion Flame in the Aluminum Anode Baking Furnace Employing Presumed PDF. Energy Procedia. 2017 Dec 31; 142:4157-62.
[14] Zaidani M, Al-Rub RA, Tajik AR, Shamim T. 3D Multiphysics model of the effect of flue-wall deformation on the anode baking homogeneity in horizontal flue carbon furnace. Energy Procedia. 2017 Dec 31; 142:3982-9.
[15] Tajik AR, Shamim T, Ghoniem AF, Abu Al-Rub RK. CFD Modelling of NOx and Soot Formation in Aluminum Anode Baking Furnace. In. ASME's International Mechanical Engineering Congress and Exposition (IMECE), 2018. Paper No. IMECE2018-88390, pp. V08AT10A016; 8 pages.